

Branching Fractions and Direct CP Asymmetries of Charmless B Decay Modes at CDF

Michal Kreps^{1a} on behalf of the CDF Collaboration

Institute für Experimentelle Kernphysik, Universität Karlsruhe (TH), Postfach 6980, 76128 Karlsruhe, Germany

Abstract. We present new CDF results on the branching fractions and time-integrated direct CP asymmetries for B^0 and B_s^0 decay modes into pairs of charmless charged hadrons (pions or kaons). The data-set for this update amounts to 1 fb^{-1} of $p\bar{p}$ collisions at a center of mass energy 1.96 TeV. We report the first observation of the $B_s \rightarrow K^- \pi^+$ mode and a measurement of its branching fraction and direct CP asymmetry. We also observe for the first time two charmless decays of the Λ_b^0 -baryon: $\Lambda_b^0 \rightarrow p\pi^-$ and $\Lambda_b^0 \rightarrow pK^-$.

PACS. 13.25.Hw Decays of bottom mesons – 14.40.Nd Bottom mesons

1 Introduction

The decay modes of B mesons into pairs of charmless pseudo-scalar mesons are effective probes of the CKM matrix with sensitivity to potential new physics. The production cross section of B hadrons at the Tevatron allows studies of such decays which are competitive to B factories. In addition B hadrons of all kind are produced at the Tevatron and thus making possible to complement the information by studies of decays of B_s mesons and B baryons which is impossible at current B factories.

In this paper we review current results on charmless two body decays of B hadrons from the CDF experiment using 1 fb^{-1} of data. We use charged kaons, pions and protons as final state particles. The main results presented here are the first observation of the decay $B_s^0 \rightarrow K^- \pi^+$ and measurement of direct CP asymmetries in $B^0 \rightarrow K^+ \pi^-$ and $B_s^0 \rightarrow K^- \pi^+$ decays. The presented analysis is an update of the previous result obtained with 360 pb^{-1} of data [1] and more details about it can be found in the Ref. [2].

2 Data sample

We analyze a data sample with an integrated luminosity of 1 fb^{-1} collected by the CDF II detector at Tevatron. Online selection of events requires two oppositely charged tracks, each with $p_T > 2 \text{ GeV}/c$. The scalar sum $p_T(1) + p_T(2)$ is required to be larger than $5.5 \text{ GeV}/c$ and the transverse opening angle between tracks ranges from 20° to 135° . The CDF detector has the unique opportunity to use the silicon tracking at trigger level. This allows us to place requirements on

the impact parameter d_0 of each track and on the displacement of the secondary vertex L_{xy} . We use $100 \mu\text{m} < d_0 < 1 \text{ mm}$ for the two tracks, $d_0 < 140 \mu\text{m}$ and $L_{xy} > 200 \mu\text{m}$ for the B hadron candidate.

The offline selection is done using pseudoexperiments with statistical uncertainty of the studied quantity as a figure of merit. During the optimization, the requirements from the trigger level are tightened. In addition to tightening trigger cuts we add other two discriminating variables, which are the quality of the B secondary candidate vertex fit and the isolation defined as $I(B) = p_T(B)/[p_T(B) + \sum_i p_T(i)]$, where the sum runs over all tracks not associated with the B candidate in a cone of unit radius in the η - ϕ space around the B candidate. As a result we derive two sets of requirements, one optimized for measurements in decay modes with larger yields and the other one for measurements in modes with lower yields. They optimize the sensitivity for the measurement of the CP asymmetry $A_{\text{CP}}(B^0 \rightarrow K^+ \pi^-)$ and for the discovery of the decay $B_s^0 \rightarrow K^- \pi^+$.

3 Signal decomposition

In Fig. 1 we show the typical expectation of the invariant mass distribution obtained from simulated events assigning pion mass to both decay products. Despite the excellent mass resolution on the level of $22 \text{ MeV}/c^2$ it is not possible to distinguish different decays as separate peaks in the invariant mass distribution. In addition the particle identification system of the CDF detector does not allow track-by-track identification.

To find out the composition of the signal an unbinned maximum likelihood fit is performed using the invariant $\pi\pi$ mass $M_{\pi\pi}$, dE/dx measurement and momenta of the two tracks. The fit determines fractions

^a Email: kreps@ekp.uni-karlsruhe.de

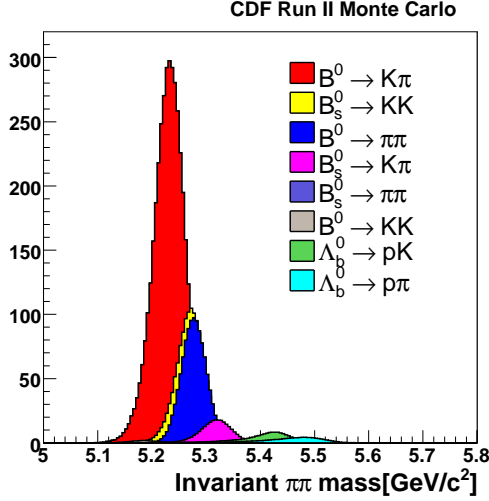


Fig. 1. Expected invariant mass distribution for different charmless two-body decays of B hadrons. In all cases the invariant mass distribution is calculated assigning pion mass to both decay products.

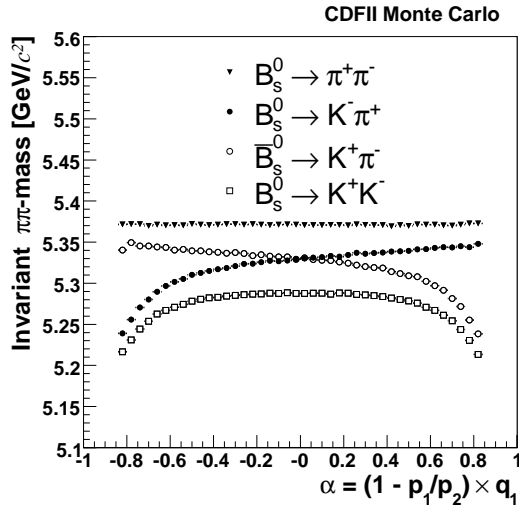


Fig. 2. Average $M_{\pi\pi}$ versus α for simulated B_s^0 decays. Corresponding dependencies for other B hadrons are analogous.

of different components, which are then converted to physical quantities like branching fractions and CP asymmetries. The momenta of the two tracks enters in a form of loosely correlated variables $p_{tot} = p_1 + p_2$ and $\alpha = (1 - p_1/p_2)q_1$ where index 1 (2) corresponds to particle with lower (higher) momentum. The invariant mass with correct mass assignment to the daughters can be unambiguously calculated from $M_{\pi\pi}$ and momenta of the two daughters. The dependence of the $M_{\pi\pi}$ on the α for B_s^0 decays is shown in Fig. 2. Decays of other three B hadrons have similar dependencies. The likelihood used in the fit has the form

$$\mathcal{L}_i = (1 - b) \sum_j f_j \mathcal{L}_j^{\text{kin}} \mathcal{L}_j^{\text{PID}} + b (f_A \mathcal{L}_A^{\text{kin}} \mathcal{L}_A^{\text{PID}} + (1 - f_A) \mathcal{L}_E^{\text{kin}} \mathcal{L}_E^{\text{PID}}) \quad (1)$$

where b is a background fraction and indices A and E label physics and combinatorial background. Index j runs over signal B^0 , B_s^0 and Λ_b^0 decays modes. \mathcal{L}^{kin} (\mathcal{L}^{PID}) denotes the mass (particle identification) part of the likelihood. The background mass distribution is described by an Argus function convoluted with a Gaussian for physics background and an exponential function for combinatorial background.

The need of disentangling of many overlapping signal contributions demands a good description of the signal PDF distributions in the likelihood fit. One of the main effects for the mass description is the inclusion of a tail due to the final state radiation. This is modeled using QED calculations [3]. The result is then convoluted with the resolution function obtained from simulated events. The description is found to be in excellent agreement with $D^0 \rightarrow K^- \pi^+$ decays from $D^{*+} \rightarrow D^0 \pi^+$ decays reconstructed in the data.

For a proper description of the particle identification, we calibrate the dE/dx response using a data sample of $D^{*+} \rightarrow D^0 \pi^+$ with $D^0 \rightarrow K^- \pi^+$, which provides a very clean sample of kaons and pions. On this sample we obtain a separation between kaons and pions around 1.4σ . After the calibration we use the same data sample to derive the probability density function for the likelihood. This is the same for signal and background except of fractions of different particles, which are independent for signal and background.

4 Results

The result of the analysis is a refined measurement of several ratios of branching fractions for previously observed decays. More important new decay modes $B_s^0 \rightarrow K^- \pi^+$, $\Lambda_b^0 \rightarrow pK^-$ and $\Lambda_b^0 \rightarrow p\pi^-$ are observed here for the first time. The invariant mass distribution using a set of tighter requirements optimized for the observation of the $B_s^0 \rightarrow K^- \pi^+$ is shown in Fig. 3. Measured ratios of the branching fractions for all observed decay modes are summarized in Table 1. The dominant systematic uncertainties are due to the statistical uncertainty on selection efficiency, the uncertainty on the dE/dx calibration and parametrization and the uncertainty on the background modeling. In the following we will concentrate in more details on the two results, which are the measurement of the $B^0 \rightarrow K^+ \pi^-$ CP asymmetry and the observation of the $B_s^0 \rightarrow K^- \pi^+$ decay and measurement of the corresponding direct CP asymmetry.

4.1 $B^0 \rightarrow K^+ \pi^-$ CP asymmetry

As the decay $B^0 \rightarrow K^+ \pi^-$ is self tagging, one can measure the direct CP asymmetry defined as

$$A_{\text{CP}} = \frac{N(\bar{B}^0 \rightarrow K^- \pi^+) - N(B^0 \rightarrow K^+ \pi^-)}{N(\bar{B}^0 \rightarrow K^- \pi^+) + N(B^0 \rightarrow K^+ \pi^-)} \quad (2)$$

The only significant difference between B^0 and \bar{B}^0 from the efficiency point of view is the difference in

Table 1. Results on the data sample optimized to measure $A_{CP}(B^0 \rightarrow K^+\pi^-)$ (top) and $\mathcal{B}(B_s^0 \rightarrow K^-\pi^+)$ (bottom). Absolute branching fractions are normalized to the the world-average values $\mathcal{B}(B^0 \rightarrow K^+\pi^-) = (19.7 \pm 0.6) \times 10^{-6}$ and $f_s = (10.4 \pm 1.4)\%$ and $f_d = (39.8 \pm 1.0)\%$ [4]. The first quoted uncertainty is statistical, the second is systematic. N_s is the number of fitted events for each mode. For rare modes both the systematic and statistical uncertainty on N_s was quoted while for abundant modes only the statistical one. For the Λ_b^0 modes only the ratio $\frac{\mathcal{B}(\Lambda_b^0 \rightarrow p\pi^-)}{\mathcal{B}(\Lambda_b^0 \rightarrow pK^-)}$ was measured.

Mode	N_s	Quantity	Measurement	$\mathcal{B}(10^{-6})$
$B^0 \rightarrow K^+\pi^-$	4045 ± 84	$\frac{\mathcal{B}(\overline{B}^0 \rightarrow K^-\pi^+) - \mathcal{B}(B^0 \rightarrow K^+\pi^-)}{\mathcal{B}(\overline{B}^0 \rightarrow K^-\pi^+) + \mathcal{B}(B^0 \rightarrow K^+\pi^-)}$	$-0.086 \pm 0.023 \pm 0.009$	
$B^0 \rightarrow \pi^+\pi^-$	1121 ± 63	$\frac{\mathcal{B}(B^0 \rightarrow \pi^+\pi^-)}{\mathcal{B}(B^0 \rightarrow K^+\pi^-)}$	$0.259 \pm 0.017 \pm 0.016$	$5.10 \pm 0.33 \pm 0.36$
$B_s^0 \rightarrow K^+K^-$	1307 ± 64	$\frac{f_s}{f_d} \frac{\mathcal{B}(B_s^0 \rightarrow K^+K^-)}{\mathcal{B}(B^0 \rightarrow K^+\pi^-)}$	$0.324 \pm 0.019 \pm 0.041$	$24.4 \pm 1.4 \pm 4.6$
$B_s^0 \rightarrow K^-\pi^+$	$230 \pm 34 \pm 16$	$\frac{f_s}{f_d} \frac{\mathcal{B}(B_s^0 \rightarrow K^-\pi^+)}{\mathcal{B}(B^0 \rightarrow K^+\pi^-)}$	$0.066 \pm 0.010 \pm 0.010$	$5.0 \pm 0.75 \pm 1.0$
		$\frac{\mathcal{B}(\overline{B}_s^0 \rightarrow K^+\pi^-) - \mathcal{B}(B_s^0 \rightarrow K^-\pi^+)}{\mathcal{B}(\overline{B}_s^0 \rightarrow K^+\pi^-) + \mathcal{B}(B_s^0 \rightarrow K^-\pi^+)}$	$0.39 \pm 0.15 \pm 0.08$	
		$\frac{f_d}{f_s} \frac{\Gamma(\overline{B}^0 \rightarrow K^-\pi^+) - \Gamma(B^0 \rightarrow K^+\pi^-)}{\Gamma(\overline{B}^0 \rightarrow K^+\pi^-) - \Gamma(B^0 \rightarrow K^-\pi^+)}$	$-3.21 \pm 1.60 \pm 0.39$	
$B_s^0 \rightarrow \pi^+\pi^-$	$26 \pm 16 \pm 14$	$\frac{f_s}{f_d} \frac{\mathcal{B}(B_s^0 \rightarrow \pi^+\pi^-)}{\mathcal{B}(B^0 \rightarrow K^+\pi^-)}$	$0.007 \pm 0.004 \pm 0.005$	$0.53 \pm 0.31 \pm 0.40$ (< 1.36 @ 90% CL)
$B^0 \rightarrow K^+K^-$	$61 \pm 25 \pm 35$	$\frac{\mathcal{B}(B^0 \rightarrow K^+K^-)}{\mathcal{B}(B^0 \rightarrow K^+\pi^-)}$	$0.020 \pm 0.008 \pm 0.006$	$0.39 \pm 0.16 \pm 0.12$ (< 0.7 @ 90% CL)
$\Lambda_b^0 \rightarrow pK^-$	$156 \pm 20 \pm 11$	$\frac{\mathcal{B}(\Lambda_b^0 \rightarrow pK^-)}{\mathcal{B}(\Lambda_b^0 \rightarrow p\pi^-)}$	$0.66 \pm 0.14 \pm 0.08$	
$\Lambda_b^0 \rightarrow p\pi^-$	$110 \pm 18 \pm 16$			

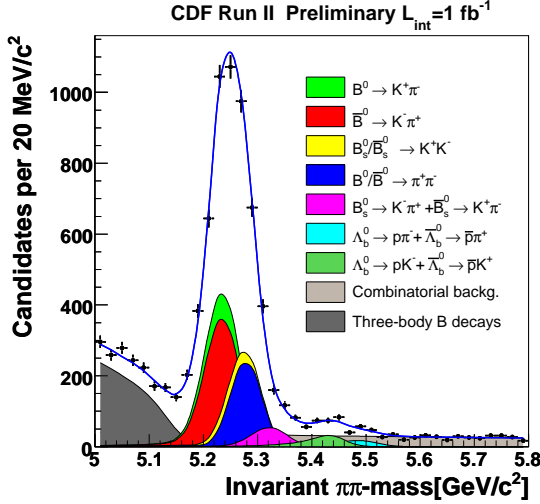


Fig. 3. Invariant mass distribution using selection optimized for $B_s^0 \rightarrow K^-\pi^+$ observation. The full line represents result of the fit.

the interaction of K^+ and K^- with detector material. This difference is estimated using a sample of prompt $D^0 \rightarrow K^-\pi^+$ decays and results in a $\leq 0.6\%$ shift for the A_{CP} obtained from the fit result. To visualize the difference between B^0 and \overline{B}^0 in Fig. 4 we show the distribution of the probability ratio $\mathcal{L}_{s1}/(\mathcal{L}_{s1} + \mathcal{L}_{s2})$ where \mathcal{L}_{s1} (\mathcal{L}_{s2}) denotes the probability to be B^0 (\overline{B}^0). The points show data while histograms represent different fit components. A small difference between B^0 and \overline{B}^0 is clearly visible. The result corrected for detector effects is $A_{CP} = -0.086 \pm 0.023 \pm 0.009$. In Fig. 5 we show a comparison of this measurement to the other existing measurements [5,6,7]. Our result is

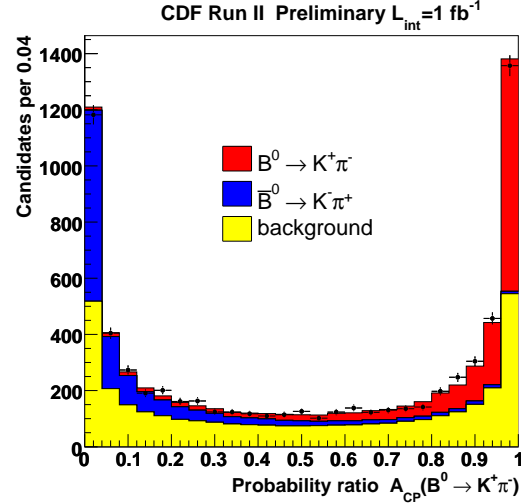


Fig. 4. Distribution of the probability ratio $\mathcal{L}_{s1}/(\mathcal{L}_{s1} + \mathcal{L}_{s2})$ where \mathcal{L}_{s1} (\mathcal{L}_{s2}) denotes the probability to be B^0 (\overline{B}^0). The points show data while histograms represent different fit components.

in good agreement with other measurements with a precision comparable to the Belle and BABAR experiments.

4.2 $B_s^0 \rightarrow K^-\pi^+$ branching fraction and CP asymmetry

The most important result obtained here, is the first observation of the decay $B_s^0 \rightarrow K^-\pi^+$. We observe $230 \pm 34 \pm 16$ signal events from which we measure

$$\frac{f_s}{f_d} \frac{\mathcal{B}(B_s^0 \rightarrow K^-\pi^+)}{\mathcal{B}(B^0 \rightarrow K^+\pi^-)} = 0.066 \pm 0.010 \pm 0.010. \quad (3)$$

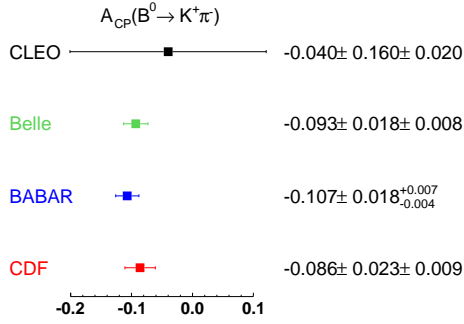


Fig. 5. Comparison of the measured $A_{CP}(B^0 \rightarrow K^+\pi^-)$ with other measurements [5, 6, 7].

The significance of the observed signal is 8.2σ including systematic uncertainties. Using world average values for f_s , f_d and $\mathcal{B}(B^0 \rightarrow K^+\pi^-)$ [4] we obtain for the branching fraction $\mathcal{B}(B_s^0 \rightarrow K^-\pi^+) = (5.0 \pm 0.75 \pm 1.0) \cdot 10^{-6}$ which is in agreement with the latest theoretical predictions [8].

As the decay $B_s^0 \rightarrow K^-\pi^+$ is a self-tagging decay, we can determine also the direct CP asymmetry. The CDF experiment has the unique opportunity for a model independent test for new physics by comparing $A_{CP}(B^0 \rightarrow K^+\pi^-)$ with $A_{CP}(B_s^0 \rightarrow K^-\pi^+)$. In the standard model one expects for the decay rate differences [9]

$$\frac{\Gamma(\overline{B}^0 \rightarrow K^-\pi^+) - \Gamma(B^0 \rightarrow K^+\pi^-)}{\Gamma(B_s^0 \rightarrow K^-\pi^+) - \Gamma(\overline{B}_s^0 \rightarrow K^+\pi^-)} = 1. \quad (4)$$

This can be used to predict $A_{CP}(B_s^0 \rightarrow K^-\pi^+)$ from the known $A_{CP}(B^0 \rightarrow K^+\pi^-)$, ratios of branching fractions and lifetimes. Using world average values provided by HFAG [4] one gets $A_{CP}(B_s^0 \rightarrow K^-\pi^+) \approx +37\%$. In Fig. 6 we show the probability ratio of being B_s^0 or \overline{B}_s^0 . We measure $A_{CP}(B_s^0 \rightarrow K^-\pi^+) = +0.39 \pm 0.15 \pm 0.08$ with 2.5σ significance. While not statistically significant, this result starts to indicate for the first time a possible direct CP violation in the B_s^0 system. The size and the sign of the measured asymmetry is in good agreement with the standard model expectation.

5 Conclusions

We presented here the latest result on the charmless two-body decays of B hadrons from the CDF experiment. We measure $A_{CP}(B^0 \rightarrow K^+\pi^-)$ which is in agreement with other measurements and has a comparable uncertainty. More important we observed three new decays which are $B_s^0 \rightarrow K^-\pi^+$, $A_b^0 \rightarrow pK^-$ and $A_b^0 \rightarrow p\pi^-$. For the decay $B_s^0 \rightarrow K^-\pi^+$ we measure also the direct CP asymmetry which for the first time starts to reveal an indication of direct CP violation in the B_s system.

While we already obtained important results, there is lot of progress to be expected in this area. First

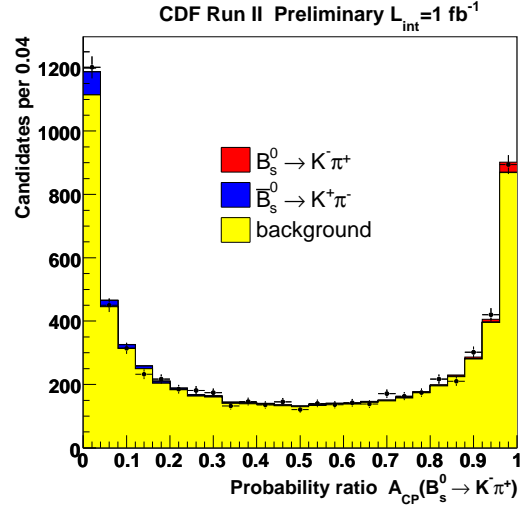


Fig. 6. Distribution of the probability ratio $\mathcal{L}_{s1}/(\mathcal{L}_{s1} + \mathcal{L}_{s2})$ where \mathcal{L}_{s1} (\mathcal{L}_{s2}) denotes the probability to be B_s^0 (\overline{B}_s^0). The points show data while histograms represent different fit components.

of all, we already collected 2.5 fb^{-1} of data, which is a substantial increase compared to data used in the presented results. With this increase in the available statistics we expect not only a decrease of the statistical uncertainties, but also the systematic uncertainties as in many cases the dominant systematic uncertainties come from the limited statistics of the control data samples. Finally a large sample of $B_s^0 \rightarrow K^+K^-$ decays is interesting for the lifetime measurement and tagged time dependent measurements.

Acknowledgments

The author would like to thank the members of the CDF Collaboration who performed the analysis as well to those who helped to improve the presentation of this interesting result.

References

1. A. Abulencia *et al.* [CDF Collaboration], Phys. Rev. Lett. **97** (2006) 211802 [arXiv:hep-ex/0607021].
2. CDF Collaboration, CDF Public Note 8579.
3. E. Baracchini and G. Isidori, Phys. Lett. B **633**, (2006) 309, [arXiv:hep-ph/0508071].
4. E. Barberio *et al.*, Heavy Flavor Averaging Group (HFAG), arXiv:hep-ex/0603003.
5. S. Chen *et al.* [CLEO Collaboration], Phys. Rev. Lett. **85** (2000) 525 [arXiv:hep-ex/0001009].
6. Belle Collaboration, talk by Y. Unno presented at ICHEP06 (2006).
7. B. Aubert *et al.* [BABAR Collaboration], Phys. Rev. Lett. **99** (2007) 021603 [arXiv:hep-ex/0703016].
8. A. R. Williamson and J. Zupan, Phys. Rev. D **74** (2006) 014003 [Erratum-ibid. D **74** (2006) 03901] [arXiv:hep-ph/0601214].
9. M. Gronau and J. L. Rosner, Phys. Lett. B **482** (2000) 71 [arXiv:hep-ph/0003119].